Electron-impact excitation of electric octupole transitions in positive ions: Asymptotic behavior of the sum over partial-collision strengths

M. C. Chidichimo
Department of Applied Mathematics, University of Waterloo, Waterloo, Ontario, Canada N2L 3G1
(Received 28 November 1990; revised manuscript received 1 April 1991)

An investigation has been made, for the case of octupole transitions, of the dependence of the partial-collision strength on the orbital angular momentum of the colliding electron. It is shown that, similar to the dipole and quadrupole transitions, the sum over partial-collision strengths is asymptotic to a geometric series of common ratio E_j/E_i, where E_i and E_j are the initial and final energies of the colliding electron, respectively. For large incident energies ($E_j/E_i \sim 1$) the convergence of the sum to the geometric series is rather slow, since the geometric-series method only starts to become valid for large values of angular momentum. This difficulty is overcome by developing an alternative method in which the approximation is made that $E_j/E_i = 1$. An analytic formula is then obtained to estimate the contribution to the total-collision strength from large values of angular momentum. Results of partial- and total-collision strengths are presented for direct electric octupole transitions in Ca^+ and Sr^+.

PACS number(s): 34.80.Kw, 34.80.Dp

I. INTRODUCTION

Optically forbidden $E3$-type transitions in positive ions [1,2] may be excited by electron impact. It is already known that in the case of dipole [3,4] and quadrupole [5] transitions the sums of partial-collision strengths are asymptotic to a geometric series with common ratio E_j/E_i. The object of this paper is to show that octupole transitions follow the same pattern; and the sum of partial-collision strengths, for a colliding electron angular momentum $l \gg E_j/(E_i - E_j)$, is also asymptotic to a geometric series with the same common ratio E_j/E_i, where E_i and E_j are the initial and final energies of the colliding electron, respectively. As E_i increases, the ratio $E_j/E_i \sim 1$ and the convergence of the sum to the geometric series is rather slow. In this case a different method is implemented to complete the sum. The approximation used in this procedure is $E_j/E_i = 1$, and consequently several expressions from the general theory of Coulomb excitation reduce appreciably. It is shown that for l large, terms in the infinite sum decrease as l^{-5}, l^{-6}, and l^{-7}. The collision problem has been formulated in atomic units, except for energies where we have used Rydberg units.

II. THEORY

The initial work closely follows that of a previous paper [5]. We give, without derivation, the expressions used in calculating the dimensionless quantity collision strength for electron-impact excitation of positive ions. The total-collision strength $\Omega(nl_a \rightarrow n'l'_a)$ has the partial-wave expansion

$$\Omega(nl_a \rightarrow n'l'_a) = \sum_{l,l'} \Omega_{l'l} \ , \tag{1}$$

where nl_a and $n'l'_a$ are the initial and final target states, and l and l' are the initial and final quantum numbers for the angular momentum of the colliding electron. The expression for $\Omega_{l'l}$ in terms of the transmission matrix $\underline{T}$ is given by

$$\Omega_{l'l} = \sum_{S=0,1} \sum_{L} \tfrac{1}{2}(2S+1)|T(n'l'_a k'l'LS, nl_a kl, LS)|^2 \ , \tag{2}$$

where k and k' are the wave numbers of the incident and scattered electron, respectively, and L and S the conserved total angular momenta and total spin quantum number, respectively. The transmission matrix $\underline{T}$ is of block-diagonal type with each block corresponding to a given LS symmetry for the total system (i.e., target ion plus colliding electron).

The infinite sum in Eq. (1) is split into two parts

$$\Omega(nl_a \rightarrow n'l'_a) = \Omega_{l_0} + \tilde{\Omega}_{l_0+1} \ , \tag{3}$$

where

$$\Omega_{l_0} = \sum_{l=0}^{l_0} \sum_{l'} \Omega_{l'l} \ , \tag{4}$$

and

$$\tilde{\Omega}_{l_0+1} = \sum_{l=l_0+1}^{\infty} \sum_{l'} \Omega_{l'l}^{\mathrm{CBeI}} \ . \tag{5}$$

The sum from $l = 0$ to l_0 may be evaluated in any desired approximation, e.g., R-matrix method, close coupling, Coulomb distorted wave, etc. The sum from $l = l_0 + 1$ to ∞ is estimated using the Coulomb Bethe weak-coupling approximation (CBeI) to the transmission matrix. In the limit of large l the ratio $(\Omega_{l'l}/\Omega_{l'l}^{\mathrm{CBeI}}) \sim 1$, and then l_0 is chosen so that this condition is fulfilled. Since relativistic effects have been neglected in the collision Hamiltonian and the effect of exchange between the colliding and bound electron is negligible when l_0 is large, the transmission matrix $\underline{T}$ does not depend on S and

$$\Omega_{l'l}^{\mathrm{CBeI}} = 2 \sum_{L} (2L+1)|T^{\mathrm{CBeI}}(n'l'_a k'l'L, nl_a klL)|^2 \ . \tag{6}$$

Standard techniques of Racah algebra reduce the previous expression to

$$\Omega_{l'l}^{\mathrm{CBeI}} = 32(2l_a+1)(2l'_a+1)(2l+1)(2l'+1) \times \sum_{\lambda} \frac{(C_{000}^{l_a l'_a \lambda} C_{000}^{l l' \lambda})^2}{(2\lambda+1)^3} (z-1)^{2\lambda-2} \times B^2(nl_a, n'l'_a;\lambda) I^2(\kappa l, \kappa' l';\lambda) , \quad (7)$$

where $C_{000}^{l_a l'_a \lambda}$ and $C_{000}^{l l' \lambda}$ are Clebsch-Gordan coefficients [6], λ satisfies the selection rules $|l-l'| \le \lambda \le l+l'$ and $|l_a - l'_a| \le \lambda \le l_a + l'_a$, and $(z-1)$ is the ion charge. The integral $B(nl_a, n'l'_a;\lambda)$ is given by

$$B(nl_a, n'l'_a;\lambda) = \int_0^\infty P_{nl_a}(r) r^\lambda P_{n'l'_a}(r) dr , \quad (8)$$

where P_{nl_a} and $P_{n'l'_a}$ are the radial wave functions of the initial and final states of the atomic system. Details regarding the numerical evaluation of these single orbital wave functions have been given elsewhere [5]. The Coulomb integrals $I(\kappa l, \kappa' l';\lambda)$ are defined as

$$I(\kappa l, \kappa' l';\lambda) = \int_0^\infty \mathcal{F}(\kappa l|\rho) \mathcal{F}(\kappa' l'|\rho) \rho^{-\lambda-1} d\rho , \quad (9)$$

where

$$\mathcal{F}(\kappa l|\rho) = (z-1)^{1/2} F_{kl}(r) \quad (10)$$

and

$$\kappa = \frac{k}{(z-1)} \quad \text{and} \quad \rho = (z-1)r . \quad (11)$$

The Coulomb functions F_{kl} are subject to the boundary conditions

$$F_{kl}(0) = 0 \quad (12)$$

and

$$F_{kl}(r) \underset{r\to\infty}{\sim} k^{-1/2} \sin\left[kr + \frac{(z-1)}{k}(2kr) - \frac{l\pi}{2} + \sigma_l \right] , \quad (13)$$

with

$$\sigma_l = \arg\Gamma\left[l+1-i\frac{(z-1)}{k} \right] . \quad (14)$$

A. Electric-octupole- ($E3$-) type transitions

For transitions between target states involving $\lambda \ge 3$ and considering only the lowest multiple order $\lambda = 3$, Eq. (7) reduces to

$$\Omega_{l'l}^{\mathrm{CBeI}} = \tfrac{120}{7}(z-1)^4 B^2(nl_a, n'l'_a;3) \times \frac{l_{a>}(l_{a>}-1)(l_{a>}-2)}{(2l_{a>}-1)(2l_{a>}-3)} \frac{(l_>+1)l_>(l_>-1)}{(2l_>-3)(2l_>+3)} \times I^2(\kappa l, \kappa' l';3), \quad l' = l \pm 1 \quad (15)$$

and

$$\Omega_{l'l}^{\mathrm{CBeI}} = \tfrac{200}{7}(z-1)^4 B^2(nl_a, n'l'_a;3) \times \frac{l_{a>}(l_{a>}-1)(l_{a>}-2)}{(2l_{a>}-1)(2l_{a>}-3)} \frac{l_>(l_>-1)(l_>-2)}{(2l_>-1)(2l_>-3)} \times I^2(\kappa l, \kappa' l';3), \quad l' = l \pm 3 , \quad (16)$$

where $l_{a>}$ and $l_>$ are the greater of l_a and l'_a and of l and l', respectively.

Using Eqs. (15) and (16) in Eq. (5), $\tilde{\Omega}_{l_0+1}$ reduces to

$$\tilde{\Omega}_{l_0+1} = \tfrac{40}{7}(z-1)^4 B^2(nl_a, n'l'_a;3) \times \frac{l_{a>}(l_{a>}-1)(l_{a>}-2)}{(2l_{a>}-1)(2l_{a>}-3)} S_{l_0+1} , \quad (17)$$

where

$$S_{l_0+1} = \sum_{l=l_0+1}^{\infty} \left[3\frac{(l+1)l(l-1)}{(2l-3)(2l+3)} I^2(\kappa l, \kappa' l-1;3) + 3\frac{(l+2)(l+1)l}{(2l-1)(2l+5)} I^2(\kappa l, \kappa' l+1;3) + 5\frac{l(l-1)(l-2)}{(2l-1)(2l-3)} I^2(\kappa l, \kappa' l-3;3) + 5\frac{(l+3)(l+2)(l+1)}{(2l+5)(2l+3)} I^2(\kappa l, \kappa' l+3;3) \right] . \quad (18)$$

B. Limit of large orbital angular momentum

1. Geometric-series method

In the limit of large angular momentum ($l \gg 1$) the Coulomb integral becomes [7]

$$I(\kappa l, \kappa' l';\lambda) \sim \exp\left[\frac{\pi}{2}|\eta - \eta'| \right] I_0(\kappa l, \kappa' l';\lambda) , \quad (19)$$

where

$$\eta = \frac{1}{\kappa}, \quad \eta' = \frac{1}{\kappa'} , \quad (20)$$

and $I_0(\kappa l,\kappa' l',\lambda)$ is the integral in Eq. (9) evaluated in the Born approximation. The radial wave functions $\mathcal{F}(\kappa l|\rho)$ are in this case related to the spherical Bessel functions. The connection is given through the relation

$$\mathcal{F}(\kappa l|\rho)=\sqrt{\kappa\rho}\,j_l(\kappa\rho)\ . \tag{21}$$

By employing the further relation

$$j_l(\kappa\rho)=\left[\frac{\pi}{2\kappa\rho}\right]^{1/2}J_{l+1/2}(\kappa\rho)\ , \tag{22}$$

between the spherical Bessel functions and ordinary Bessel functions one obtains

$$I_0(\kappa l,\kappa' l';\lambda)=\frac{\pi}{2}\int_0^\infty J_{l+1/2}(\kappa\rho)J_{l'+1/2}(\kappa'\rho)\rho^{-\lambda}d\rho\ . \tag{23}$$

The integral is of the Weber-Schafheitlin type and has a discontinuity in the expressions for I_0 at $\kappa=\kappa'$. Using the analytic continuation of the ${}_2F_1$ Gauss hypergeometric function given by

$${}_2F_1(a,b;c;w)=(1-w)^{-b}\,{}_2F_1\left[c-a,b;c;\frac{w}{w-1}\right]\ , \tag{24}$$

one readily finds from Watson [8] that for $0<\kappa'<\kappa$

$$I_0(\kappa l,\kappa' l';\lambda)=\frac{\pi}{2^{\lambda+1}}\left[\frac{\kappa'}{\kappa}\right]^{l'+1/2}\kappa^{\lambda-1}\left[\frac{\kappa^2-\kappa'^2}{\kappa^2}\right]^{-[(l'-l-\lambda+1)/2]}\frac{\Gamma((l+l'-\lambda+2)/2)}{\Gamma(l'+\frac{3}{2})\Gamma((l-l'+\lambda+1)/2)}$$
$$\times{}_2F_1\left[\frac{l'-l+\lambda+1}{2},\frac{l'-l-\lambda+1}{2};l'+\tfrac{3}{2};\frac{\kappa'^2}{\kappa'^2-\kappa^2}\right]\ , \tag{25}$$

and for $0<\kappa<\kappa'$

$$I_0(\kappa l,\kappa' l';\lambda)=\frac{\pi}{2^{\lambda+1}}\left[\frac{\kappa}{\kappa'}\right]^{l+1/2}\kappa'^{(\lambda-1)}\left[\frac{\kappa'^2-\kappa^2}{\kappa'^2}\right]^{-[(l-l'-\lambda+1)/2]}\frac{\Gamma((l+l'-\lambda+2)/2)}{\Gamma(l+\frac{3}{2})\Gamma((l'-l+\lambda+1)/2)}$$
$$\times{}_2F_1\left[\frac{l-l'+\lambda+1}{2},\frac{l-l'-\lambda+1}{2};l+\tfrac{3}{2};\frac{\kappa^2}{\kappa^2-\kappa'^2}\right]\ . \tag{26}$$

Substituting $\lambda=3$ into Eqs. (25) and (26) it is shown that

$$I_0(\kappa l,\kappa' l-1;3)=\frac{\pi}{16}\left[\frac{\kappa_<}{\kappa_>}\right]^{l+1/2-p}\kappa_>^2\left[\frac{\kappa_>^2-\kappa_<^2}{\kappa_>^2}\right]^{1/2+p}\frac{\Gamma(l-1)}{\Gamma(l+\frac{3}{2}-p)\Gamma(\frac{3}{2}+p)}$$
$$\times{}_2F_1\left[\frac{5}{2}-p,-\frac{1}{2}-p;l+\frac{3}{2}-p;\frac{\kappa_<^2}{\kappa_<^2-\kappa_>^2}\right]\ , \tag{27}$$

$$I_0(\kappa l,\kappa' l+1;3)=\frac{\pi}{16}\left[\frac{\kappa_<}{\kappa_>}\right]^{l+1/2+p}\kappa_>^2\left[\frac{\kappa_>^2-\kappa_<^2}{\kappa_>^2}\right]^{3/2-p}\frac{\Gamma(l)}{\Gamma(l+\frac{3}{2}+p)\Gamma(\frac{5}{2}-p)}$$
$$\times{}_2F_1\left[\frac{3}{2}+p,-\frac{3}{2}+p;l+\frac{3}{2}+p;\frac{\kappa_<^2}{\kappa_<^2-\kappa_>^2}\right]\ , \tag{28}$$

where

$$p=\begin{cases}0 & \text{if } \kappa<\kappa'\\ 1 & \text{if } \kappa>\kappa'\ ,\end{cases}$$

and

$$I_0(\kappa l,\kappa' l-3;3)=\frac{\pi}{16}\left[\frac{\kappa_<}{\kappa_>}\right]^{l+1/2-p}\kappa_>^2\left[\frac{\kappa_>^2-\kappa_<^2}{\kappa_>^2}\right]^{-1/2+p}\frac{\Gamma(l-2)}{\Gamma(l+\frac{3}{2}-p)\Gamma(\frac{1}{2}+p)}$$
$$\times{}_2F_1\left[\frac{7}{2}-p,\frac{1}{2}-p;l+\frac{3}{2}-p;\frac{\kappa_<^2}{\kappa_<^2-\kappa_>^2}\right]\ , \tag{29}$$

$$I_0(\kappa l,\kappa' l+3;3)=\frac{\pi}{16}\left[\frac{\kappa_<}{\kappa_>}\right]^{l+1/2+p}\kappa_>^2\left[\frac{\kappa_>^2-\kappa_<^2}{\kappa_>^2}\right]^{5/2-p}\frac{\Gamma(l+1)}{\Gamma(l+\frac{3}{2}+p)\Gamma(\frac{7}{2}-p)}$$
$$\times{}_2F_1\left[\frac{1}{2}+p,-\frac{5}{2}+p;l+\frac{3}{2}+p;\frac{\kappa_<^2}{\kappa_<^2-\kappa_>^2}\right] \tag{30}$$

where

$$p=\begin{cases}0 & \text{if } \kappa<\kappa' \\ 3 & \text{if } \kappa>\kappa' \end{cases}.$$

$\kappa_<$ ($\kappa_>$) is the smaller (greater) of κ and κ'. The behavior of ${}_2F_1(a,b;c;w)$ for fixed a, b, w, and large $|c|$ is described by

$${}_2F_1(a,b;c;w)=\frac{\Gamma(c)}{\Gamma(a)\Gamma(b)}\sum_{n=0}^{m}\frac{\Gamma(a+n)\Gamma(b+n)}{\Gamma(c+n)n!}w^n+O(|c|^{-m-1}) . \tag{31}$$

Using the previous asymptotic expansion and the limit property of the Γ function

$$\lim_{n\to\infty} n^{t-s}\frac{\Gamma(n+s)}{\Gamma(n+t)}=1 , \tag{32}$$

it is possible to show that, for excitation of octupole transitions ($\kappa>\kappa'$) and l large ($l\gg\kappa_<^2/(\kappa_>^2-\kappa_<^2)\equiv E_j/(E_i-E_j)$), l-dependent terms in Eq. (18) behave as

$$\frac{5l(l-1(l-2)}{(2l-1)(2l-3)}I^2(\kappa_> l,\kappa_< l-3;3)\approx\frac{\pi}{720}\left[\frac{\kappa_<}{\kappa_>}\right]^{2l-5}\kappa_>^4\left[\frac{\kappa_>^2-\kappa_<^2}{\kappa_>^2}\right]^5 e^{\pi|\eta_>-\eta_<|} , \tag{33}$$

$$3\frac{(l+1)l(l-1)}{(2l-3)(2l+3)}I^2(\kappa_> l,\kappa_< l-1;3)\approx\frac{\pi}{192}\left[\frac{\kappa_<}{\kappa_>}\right]^{2l-1}\kappa_>^4\left[\frac{\kappa_>^2-\kappa_<^2}{\kappa_>^2}\right]^3 l^{-2}e^{\pi|\eta_>-\eta_<|} , \tag{34}$$

$$3\frac{(l+2)(l+1)l}{(2l-1)(2l+5)}I^2(\kappa_> l,\kappa_< l+1;3)\approx\frac{3\pi}{256}\left[\frac{\kappa_<}{\kappa_>}\right]^{2l+3}\kappa_>^4\left[\frac{\kappa_>^2-\kappa_<^2}{\kappa_>^2}\right] l^{-4}e^{\pi|\eta_>-\eta_<|} , \tag{35}$$

and

$$5\frac{(l+3)(l+2)(l+1)}{(2l+5)(2l+3)}I^2(\kappa_> l,\kappa_< l+3;3)\approx\frac{5\pi}{1024}\left[\frac{\kappa_<}{\kappa_>}\right]^{2l+7}\kappa_>^4\left[\frac{\kappa_>^2-\kappa_<^2}{\kappa_>^2}\right]^{-1} l^{-6}e^{\pi|\eta_>-\eta_<|} . \tag{36}$$

Substituting Eqs. (33)–(36) into S_{l_0+1} [Eq. (18)] gives

$$S_{l_0+1}\sim\frac{\pi}{720}e^{\pi|\eta_>-\eta_<|}\frac{\kappa_>^9}{\kappa_<^5}\left[\frac{\kappa_>^2-\kappa_<^2}{\kappa_>^2}\right]^5$$
$$\times\sum_{l=l_0+1}^{\infty}\left[\frac{\kappa_<^2}{\kappa_>^2}\right]^l\left[1+\frac{15}{4}\left[\frac{\kappa_>^2-\kappa_<^2}{\kappa_<^2}\right]^{-2}l^{-2}+\frac{135}{16}\left[\frac{\kappa_>^2-\kappa_<^2}{\kappa_<^2}\right]^{-4}l^{-4}+\frac{225}{64}\left[\frac{\kappa_>^2-\kappa_<^2}{\kappa_<^2}\right]^{-6}l^{-6}\right] \tag{37}$$

and for $l\gg\kappa_<^2(\kappa_>^2-\kappa_<^2)^{-1}$ the infinite sum in S_{l_0+1} is asymptotic to a geometric series of ratio $\kappa_<^2/\kappa_>^2\equiv E_j/E_i$.

Therefore the main contribution to the sum over l, in Eq. (17), arises from the partial-collision strength $\Omega^{\mathrm{CBeI}}_{l-3,l}(\kappa_<,\kappa_>)$. The completion of the summation over partial-collision strength is then straightforward and leads to the result

$$\tilde{\Omega}_{l_0+1}\sim\Omega^{\mathrm{CBeI}}_{l_0-2,l_0+1}(\kappa_<,\kappa_>)\frac{1}{(1-x)},\quad l_0\gg\frac{\kappa_<^2}{\kappa_>^2-\kappa_<^2} \tag{38}$$

where

$$x=\frac{\kappa_<^2}{\kappa_>^2}=\frac{k_<^2}{k_>^2}=\frac{E_j}{E_i} , \tag{39}$$

and E_i and E_j are the energies of the free electron before and after the collision. For an s-f transition the additional approximation is made that

$$\tilde{\Omega}_{l_0+1}\sim\Omega(nl_a\to n'l_a';L=l_0+1)/(1-x) . \tag{40}$$

2. *The method of sum of reciprocal powers*

For large incident energies, such as for, e.g., $E_j=10.924\,11$ Ry and a transition energy $E_{ij}=E_i-E_j=0.145\,51$ Ry ($5s$-$4f$ in Ca^+), $x=E_j/E_i=0.987$ or $E_j/(E_i-E_j)=75$, and the series method becomes impractical because this method is valid for partial waves $l>l_0$, where $l_0\gg E_j/(E_i-E_j)=75$. Numerical quantal calculations of partial waves [Eq. (4)] in the different approximations, R-matrix method, close coupling, Coulomb distorted wave, become prohibitive at such large values of l.

To obtain an estimate of S_{l_0+1}, at high incident electron energies, the approximation is made that $\kappa=\kappa'$ and $\bar{\kappa}^2=(\kappa^2+\kappa'^2)/2$. In this case, the octupole integrals $I(\kappa l,\kappa' l';3)$ in Eq. (18) simplify considerably [7] and reduce to

$$I(\bar{\kappa}l,\bar{\kappa}l+1;3)=\frac{\bar{\kappa}^3}{3l(l+1)(l+2)(2l+1)(2l+3)}[1+\bar{\kappa}^2(l+1)^2]^{-1/2}\times\left[\frac{6}{\bar{\kappa}^3}[1+\bar{\kappa}^2(l+1)^2]\left[\pi(1-e^{-2\pi/\bar{\kappa}})^{-1}+\bar{\kappa}^3\sum_{s=0}^{l}\frac{s^2}{1+\bar{\kappa}^2s^2}\right]-l(l+1)(2l+1)\right], \tag{41}$$

$$I(\bar{\kappa}l,\bar{\kappa}l-1;3)=\frac{\bar{\kappa}^3}{3(l-1)l(l+1)(2l-1)(2l+1)}[1+\bar{\kappa}^2l^2]^{-1/2}\times\left[\frac{6}{\bar{\kappa}^3}(1+\bar{\kappa}^2l^2)\left[\pi(1-e^{-2\pi/\bar{\kappa}})^{-1}+\bar{\kappa}^3\sum_{s=0}^{l}\frac{s^2}{1+\bar{\kappa}^2s^2}\right]-(l-1)l(2l-1)\right], \tag{42}$$

$$I(\bar{\kappa}l,\bar{\kappa}l+3;3)=\frac{\bar{\kappa}^5}{15[1+\bar{\kappa}^2(l+1)^2]^{1/2}[1+\bar{\kappa}^2(l+2)^2]^{1/2}[1+\bar{\kappa}^2(l+3)^2]^{1/2}}, \tag{43}$$

$$I(\bar{\kappa}l,\bar{\kappa}l-3;3)=\frac{\bar{\kappa}^5}{15[1+\bar{\kappa}^2(l-2)^2]^{1/2}[1+\bar{\kappa}^2(l-1)^2]^{1/2}(1+\bar{\kappa}^2l^2)^{1/2}}. \tag{44}$$

These expressions may be further simplified if the assumption is made that $l^2\bar{\kappa}^2\gg1$ and

$$\sum_{s=0}^{l}\frac{s^2}{1+\bar{\kappa}^2s^2}\approx\frac{l}{\bar{\kappa}^2}.$$

The final expression obtained for S_{l_0+1} is

$$S_{l_0+1}\approx a_5(\bar{\kappa})\sum_{l=l_0+1}^{\infty}\frac{1}{l^5}+a_6(\bar{\kappa})\sum_{l=l_0+1}^{\infty}\frac{1}{l^6}+a_7(\bar{\kappa})\sum_{l=l_0+1}^{\infty}\frac{1}{l^7}, \tag{45}$$

where

$$a_5(\bar{\kappa})=\tfrac{8}{45}\bar{\kappa}^4, \tag{46}$$

$$a_6(\bar{\kappa})=\frac{\bar{\kappa}^3\pi}{2}(1-e^{-2\pi/\bar{\kappa}})^{-1}, \tag{47}$$

$$a_7(\bar{\kappa})=\tfrac{3}{8}\bar{\kappa}^2\pi^2(1-e^{-2\pi/\bar{\kappa}})^{-2}. \tag{48}$$

The sums of reciprocal powers $\sum_{l=l_0+1}^{\infty}l^{-p}$ with $p=5,6,7$ have been calculated using the relation

$$\sum_{l=l_0+1}^{\infty}l^{-p}=\zeta(p)-\sum_{l=1}^{l_0}l^{-p} \tag{49}$$

TABLE I. CDWII partial-collision strength Ω_l, for the $4s$-$4f$ and $5s$-$4f$ transitions in Ca^+. Energy of the colliding electron after excitation E_j (Ry).

	$E_j=0.129\,11$			$E_j=1.226\,31$			$E_j=6.310\,10$	
l	$4s$-$4f$	$5s$-$4f$	l	$4s$-$4f$	$5s$-$4f$	l	$4s$-$4f$	$5s$-$4f$
9	1.514×10^{-2}	1.370	29	5.984×10^{-5}	4.012×10^{-2}	39	2.644×10^{-3}	1.037×10^{-1}
10	3.406×10^{-3}	9.000×10^{-1}	30	3.912×10^{-5}	3.380×10^{-2}	40	2.318×10^{-3}	9.246×10^{-2}
11	6.986×10^{-4}	5.182×10^{-1}	31	2.560×10^{-5}	2.860×10^{-2}	41	2.036×10^{-3}	8.258×10^{-2}
12	1.344×10^{-4}	2.746×10^{-1}	32	1.676×10^{-5}	2.428×10^{-2}	42	1.791×10^{-3}	7.386×10^{-2}
13	2.484×10^{-5}	1.383×10^{-1}	33	1.098×10^{-5}	2.066×10^{-2}	43	1.578×10^{-3}	6.618×10^{-2}
14	4.466×10^{-6}	6.752×10^{-2}	34	7.198×10^{-6}	1.765×10^{-2}	44	1.392×10^{-3}	5.938×10^{-2}
15	7.908×10^{-7}	3.234×10^{-2}	35	4.720×10^{-6}	1.511×10^{-2}	45	1.230×10^{-3}	5.338×10^{-2}
16	1.390×10^{-7}	1.531×10^{-2}	36	3.098×10^{-6}	1.297×10^{-2}	46	1.088×10^{-3}	4.808×10^{-2}
17	2.420×10^{-8}	7.196×10^{-3}	37	2.036×10^{-6}	1.116×10^{-2}	47	9.642×10^{-4}	4.338×10^{-2}
18	4.192×10^{-9}	3.368×10^{-3}	38	1.337×10^{-6}	9.618×10^{-3}	48	8.554×10^{-4}	3.922×10^{-2}
19	7.252×10^{-10}	1.572×10^{-3}	39	8.788×10^{-7}	8.306×10^{-3}	49	7.596×10^{-4}	3.552×10^{-2}
20	1.262×10^{-10}	7.320×10^{-4}	40	5.780×10^{-7}	7.186×10^{-3}	50	6.752×10^{-4}	3.224×10^{-2}
21	2.178×10^{-11}	3.408×10^{-4}	41	3.802×10^{-7}	6.228×10^{-3}	51	6.008×10^{-4}	2.930×10^{-2}

TABLE II. CDWII partial-collision strength Ω_l for the 5*s*-4*f* and 6*s*-4*f* transitions in Sr^+. Energy of the colliding electron after excitation E_j (Ry).

	$E_j=0.10513$			$E_j=1.20328$			$E_j=6.03514$	
l	5*s*-4*f*	6*s*-4*f*	l	5*s*-4*f*	6*s*-4*f*	l	5*s*-4*f*	6*s*-4*f*
9	1.433×10^{-2}	1.424	29	1.477×10^{-4}	4.744×10^{-2}	39	4.060×10^{-3}	1.104×10^{-1}
10	3.308×10^{-3}	9.656×10^{-1}	30	9.980×10^{-5}	3.946×10^{-2}	40	3.576×10^{-3}	9.850×10^{-1}
11	6.908×10^{-4}	5.846×10^{-1}	31	6.748×10^{-5}	3.360×10^{-2}	41	3.154×10^{-3}	8.796×10^{-2}
12	1.331×10^{-4}	3.252×10^{-1}	32	4.566×10^{-5}	2.874×10^{-2}	42	2.786×10^{-3}	7.864×10^{-2}
13	2.414×10^{-5}	1.701×10^{-1}	33	3.092×10^{-5}	2.466×10^{-2}	43	2.466×10^{-3}	7.044×10^{-2}
14	4.208×10^{-6}	8.546×10^{-2}	34	2.094×10^{-5}	2.122×10^{-2}	44	2.186×10^{-3}	6.320×10^{-2}
15	7.152×10^{-7}	4.174×10^{-2}	35	1.419×10^{-5}	1.833×10^{-2}	45	1.940×10^{-3}	5.678×10^{-2}
16	1.194×10^{-7}	2.002×10^{-2}	36	9.618×10^{-5}	1.587×10^{-2}	46	1.725×10^{-3}	5.112×10^{-2}
17	1.966×10^{-8}	9.494×10^{-3}	37	6.522×10^{-6}	1.378×10^{-2}	47	1.535×10^{-3}	4.610×10^{-2}
18	3.210×10^{-9}	4.466×10^{-3}	38	4.424×10^{-6}	1.200×10^{-2}	48	1.368×10^{-3}	4.166×10^{-2}
19	5.218×10^{-10}	2.092×10^{-3}	39	3.004×10^{-6}	1.047×10^{-2}	49	1.221×10^{-3}	3.772×10^{-2}
20	8.486×10^{-11}	9.764×10^{-4}	40	2.040×10^{-6}	9.156×10^{-3}	50	1.090×10^{-3}	3.420×10^{-2}
21	1.355×10^{-11}	4.548×10^{-4}	41	1.385×10^{-6}	8.024×10^{-3}	51	9.750×10^{-4}	3.106×10^{-2}

where $\zeta(p)$ is the Riemann zeta function. The calculations were carried out using the symbolic computation program MAPLE [9], to a high degree of accuracy. Hereafter S_{l_0+1} [Eq. (45)] is inserted into Eq. (17) to yield $\tilde{\Omega}_{l_0+1}$.

III. RESULTS

Results are presented for two optically forbidden *E*3-type transitions in Ca^+ and Sr^+. Collision strengths were obtained using a unitarized nonexchange Coulomb-distorted-wave (CDWII) seven-state approximation, 4*s*-3*d*-4*p*-5*s*-4*d*-5*p*-4*f* in Ca^+ and 5*s*-4*d*-5*p*-6*s*-5*d*-6*p*-4*f* in Sr^+. The target valence orbitals $P_{nl_a}(r)$ are solutions of a one-electron Schrödinger equation with observed binding energies [10]. The collision approximation assumes *LS* coupling and takes into account all open channels based on the lowest seven states of Ca^+ and Sr^+, respectively. Tables I and II contain partial-collision strengths for the excitation of the 4*s*-4*f*, 5*s*-4*f* transitions in Ca^+ and 5*s*-4*f*, 6*s*-4*f* transitions in Sr^+, respectively. The asymptotic behavior of the collision strengths for large angular momenta was checked using the data in Tables I and II. In Tables III and IV the ratio Ω_l/Ω_{l-1} has been tabulated as a function of the colliding electron angular momentum l, where $\Omega_l=\sum_{l'}\Omega_{l'l}$ for different energies of the colliding electron after excitation. For large l, $\Omega_{l'l}^{\mathrm{CDWII}}\sim\Omega_{l'l}^{\mathrm{CBeI}}$ and the ratio Ω_l/Ω_{l-1} tends to a constant $x=E_j/E_i$, where E_i and E_j are the energies of the free electron before and after excitation. Tables III and IV show results for the excitation of the 4*s*-4*f* and 5*s*-4*f* transitions in Ca^+ and excitation of the 5*s*-4*f* and 6*s*-4*f* transitions in Sr^+, respectively. Also shown are the quantities $x=E_j/E_i$ and $a=E_j/(E_i-E_j)$. These tables illustrate the fact that for large values of the electron-impact energy, and/or for transitions in which the atomic states are energetically close, e.g., the transition 5*s*-4*f* in Ca^+ and the transition 6*s*-4*f* in Sr^+, the sum over partial-collision strengths $\tilde{\Omega}_{l_0+1}$ [Eq. (5)] is slowly convergent, to a geometric series of common ratio E_j/E_i. The

TABLE III. Ω_l/Ω_{l-1} for the 4*s*-4*f* and 5*s*-4*f* transitions in Ca^+. $x=E_j/E_i$, $a=E_j/E_{ij}$. Energy of the colliding electron before excitation E_i (Ry), energy of the colliding electron after excitation E_j (Ry). Excitation energy E_{ij}(Ry)$=E_i-E_j$.

	$E_j=0.12911$			$E_j=1.22631$			$E_j=6310\,10$	
	$x=0.172$ $a\sim0.2$	$x=0.470$ $a\sim0.9$		$x=0.664$ $a\sim2$	$x=0.894$ $a\sim8$		$x=0.910$ $a\sim10$	$x=0.978$ $a\sim43$
l	4*s*-4*f*	5*s*-4*f*	l	4*s*-4*f*	5*s*-4*f*	l	4*s*-4*f*	5*s*-4*f*
10	0.225	0.657	30	0.654	0.842	40	0.877	0.892
11	0.205	0.576	31	0.654	0.846	41	0.878	0.893
12	0.192	0.530	32	0.655	0.849	42	0.879	0.894
13	0.185	0.504	33	0.655	0.851	43	0.881	0.896
14	0.180	0.488	34	0.656	0.854	44	0.882	0.897
15	0.177	0.479	35	0.656	0.856	45	0.883	0.899
16	0.176	0.474	36	0.656	0.858	46	0.885	0.901
17	0.174	0.470	37	0.657	0.860	47	0.886	0.902
18	0.173	0.468	38	0.657	0.862	48	0.887	0.904
19	0.173	0.467	39	0.657	0.864	49	0.888	0.906
20	0.174	0.466	40	0.658	0.865	50	0.889	0.908
21	0.173	0.466	41	0.658	0.867	51	0.890	0.909

TABLE IV. Ω_l/Ω_{l-1} for the $5s$-$4f$ and $6s$-$4f$ transitions in Sr^+. $x=E_j/E_i$, $a=E_j/E_{ij}$. Energy of the colliding electron before excitation E_i (Ry), energy of the colliding electron after excitation E_j (Ry). Excitation energy E_{ij}(Ry)$=E_i-E_j$.

	$E_j=0.105\,13$			$E_j=1.203\,28$			$E_j=6.035\,14$	
	$x=0.160$ $a\sim0.2$	$x=0.470$ $a\sim0.9$		$x=0.685$ $a\sim2$	$x=0.910$ $a\sim10$		$x=0.916$ $a\sim11$	$x=0.981$ ~51
l	$5s$-$4f$	$6s$-$4f$	l	$5s$-$4f$	$6s$-$4f$	l	$5s$-$4f$	$6s$-$4f$
10	0.231	0.678	30	0.676	0.832	40	0.881	0.892
11	0.209	0.605	31	0.676	0.851	41	0.882	0.893
12	0.193	0.556	32	0.677	0.855	42	0.883	0.894
13	0.181	0.523	33	0.677	0.858	43	0.885	0.896
14	0.174	0.502	34	0.677	0.861	44	0.886	0.897
15	0.170	0.488	35	0.678	0.864	45	0.888	0.898
16	0.167	0.480	36	0.678	0.866	46	0.889	0.900
17	0.165	0.474	37	0.678	0.868	47	0.890	0.902
18	0.163	0.470	38	0.678	0.870	48	0.891	0.904
19	0.163	0.468	39	0.679	0.873	49	0.892	0.905
20	0.163	0.467	40	0.679	0.874	50	0.893	0.907
21	0.160	0.466	41	0.679	0.876	51	0.894	0.908

TABLE V. CDWII total-collision strength Ω for the $5s$-$4f$ transition in Sr^+. The contributions Ω_{l_0} and $\tilde{\Omega}_{l_0+1}$ to Ω are shown separately. $\tilde{\Omega}_{l_0+1}$ has been calculated using the geometric-series method.

E_j (Ry)	l_0	Ω_{l_0}	$\tilde{\Omega}_{l_0+1}$	Ω	$\tilde{\Omega}_{l_0+1}$ as percentage of Ω
0.105 13	20	1.278	~0	1.278	~0
0.214 94	20	1.328	~0	1.328	~0
0.462 83	20	1.362	~0	1.362	~0
1.203 28	40	1.346	2.223×10^{-6}	1.346	~0
1.642 54	40	1.293	3.831×10^{-5}	1.293	~0

TABLE VI. CDWII total-collision strength Ω for the $5s$-$4f$ transition in Ca^+. The contributions Ω_{l_0} and $\tilde{\Omega}_{l_0+1}$ to Ω are shown separately, together with error estimates. $\tilde{\Omega}_{l_0+1}$ has been calculated using the reciprocal power method.

E_j (Ry)	E_j/E_i	l_0	$\Omega_{l_0}^{\mathrm{CDWII}}/\Omega_{l_0}^{\mathrm{CBeI}}$	Ω_{l_0}	$\tilde{\Omega}_{l_0+1}$	Ω	$\tilde{\Omega}_{l_0+1}$ as percentage of Ω	Percentage absolute error in Ω
6.310 10	0.977	51	0.94	14.704	3.160×10^{-1}	15.020	2	1
10.924 11	0.987	59	1.08	14.406	5.180×10^{-1}	14.924	3	1

TABLE VIII. Electric octupole integral $B(ns,nf;3)$.

	Transition	$B(a_0^4)$
Ca^+	$4s$-$4f$	−86.56
	$5s$-$4f$	712.2
Sr^+	$5s$-$4f$	115.0
	$6s$-$4f$	−770.0

geometric-series method only starts to become useful for $l > l_0$, where $l_0 \gg a = E_j/(E_i - E_j)$ and Ω_{l_0} [Eq. (4)] then requires contributions from a large number of partial waves $\Omega_{l'l}$ which are calculated in any desired quantal approximation. For colliding energies near threshold, i.e., $0.105\,13 \le E_j \le 1.642\,54$ Ry, l_0 has been chosen as the value at which $\Omega_{l_0}^{\text{CDWII}}/\Omega_{l_0-1}^{\text{CDWII}} \sim x = E_j/E_i$ within at most a 4% error. In Table V, it is shown, for the transition $5s$-$4f$ in Sr^+, for each incident electron energy and angular momentum l_0, the two contributions Ω_{l_0} (CDWII approximation) and $\tilde{\Omega}_{l_0+1}$ to the total-collision strength Ω, as well as the percentage contribution to $\tilde{\Omega}_{l_0+1}$. The quantal calculations become increasingly difficult, from the computational point of view, as the electron-impact energy and l increase. Therefore, to avoid these difficulties, the alternative method of sums of reciprocal powers [Eq. (45)] is used to estimate S_{l_0+1}.

A sample calculation, on the $5s$-$4f$ transition in Ca^+, of the contributions Ω_{l_0} and $\tilde{\Omega}_{l_0+1}$ to the total collision strength Ω is presented in Table VI. The percentage contribution of $\tilde{\Omega}_{l_0+1}$ to Ω is also shown, as well as an estimate of the percentage error in Ω due to the use of the analytic formulas (17) and (45), found by the method described below. The error estimate is only for this effect, not for the CDWII approximation which is of the order of 1%. An upper bound on the average error made by using $\tilde{\Omega}_{l_0+1}$ to complete the infinite sum may be estimated in the following way. The contribution to Ω from angular momentum l_1+1 to l_2 is denoted by $\Delta\Omega$ and is calculated by two methods. The first estimate is

$$\Delta\Omega^{\text{num}} = \sum_{l=l_1+1}^{l_2} \sum_{l'} \Omega_{l'l}^{\text{CDWII}} ,$$

which has been compared with the second estimate

$$\Delta\Omega = \tilde{\Omega}_{l_1+1} - \tilde{\Omega}_{l_2+1} ,$$

which uses the approximate formulas (17) and (45). It has been then assumed that the error thus found in $\Delta\Omega$ is constant for all $\tilde{\Omega}_l$ when $l > l_2$. This is clearly an overestimate of the total error, because Eqs. (17) and (45) represent better the contribution to the total-collision strength Ω from large angular momentum, as l increases. The percentage error in Ω is obtained by dividing the percentage error in $\tilde{\Omega}_{l_0}$ by Ω. The procedure to estimate this error is similar to the one developed for quadrupole transitions [11]. At the largest impact energy $E_j = 22.469\,11$ Ry, and for the transitions $5s$-$4f$ in Ca^+ and $6s$-$4f$ in Sr^+, an estimate of the error is more difficult since the convergence of the CDWII to the CBeI approximation has not been attained at an angular momentum as large as $l = 58$. These data points were not included in Table IX. In order to show that the geometric-series method does not give accurate results for the energies listed in Table VI, the contribution $\tilde{\Omega}_{l_0+1}$ that the method would give is presented in Table VII, together with the contribution Ω_{l_0}. The percentage contribution of $\tilde{\Omega}_{l_0+1}$ to Ω is also shown, as well as an estimate of the percentage error in Ω due to the use of formula (40). Because the contribution of $\tilde{\Omega}_{l_0+1}$ to Ω is so large for $E_j = 22.469\,11$ Ry, the scheme used to calculate the percentage error in Ω no longer applies and the error shown is undoubtedly too low. Values of the electric octupole integral $B(ns;nf;3)$ [Eq. (8)] are shown in Table VIII for both ions.

Total-collision strengths, for excitation of octupole transitions in Ca^+ and Sr^+, obtained using a unitarized seven-state CDWII approximation are given in Table IX, including values at $E_j = \infty$ obtained by the Born approximation.

In the limit of infinite electron-impact energy, the Born approximation for the collision strength of an electric oc-

TABLE IX. CDWII total-collision strengths $\Omega(ns,n'f)$ for Ca^+ and Sr^+. Energy of the colliding electron after excitation E_j (Ry). Transition energy $E_{ij}(\text{Ry}) = E_i - E_j$.

Ca^+			Sr^+		
	$4s$-$4f$	$5s$-$4f$		$5s$-$4f$	$6s$-$4f$
E_j	$E_{ij} = 0.620\,89$	$E_{ij} = 0.145\,51$	E_j	$E_{ij} = 0.553\,76$	$E_{ij} = 0.118\,50$
0.129 11	2.184	15.596	0.105 13	2.556	16.132
0.385 10	2.144	17.052	0.214 94	2.656	17.646
0.764 51	2.026	16.908	0.462 83	2.724	18.196
1.226 31	1.918	16.358	1.203 28	2.692	17.046
1.693 43	1.828	15.900	1.642 54	2.586	16.746
6.310 10	1.411	15.020	6.035 14	2.126	15.638
10.924 11	1.298	14.924	10.427 74	2.020	15.530
22.469 11	1.218		21.409 24	1.947	
∞	1.193	14.872	∞	1.936	15.477

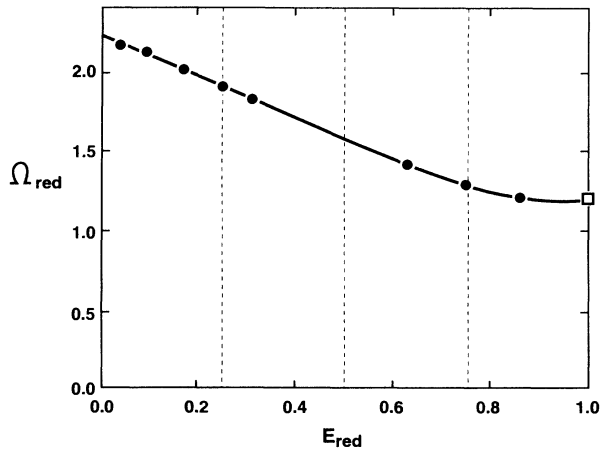

FIG. 1. Scaled total-collision strength Ω_{red} for the $4s$-$4f$ transition in Ca^+, plotted against scaled energy E_{red}. ●, reduced data; ——, spline fit to the reduced data; □, Born limit. Adjustable parameter $C=4$ with knot values 2.238, 1.919, 1.572, 1.290, 1.193.

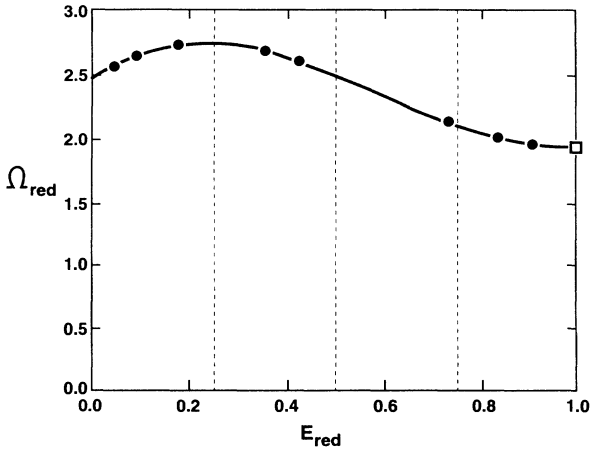

FIG. 3. Scaled total-collision strength Ω_{red} for the $5s$-$4f$ transition in Sr^+, plotted against scaled energy E_{red}. ●, reduced data; ——, spline fit to the reduced data; □, Born limit. Adjustable parameter $C=6$ with knot values 2.465, 2.75, 2.481, 2.095, 1.934.

tupole transition between $nl_a - n'l'_a$ levels can be written as

$$\Omega = C_3 I_3^{(-3)} , \tag{50}$$

where the factor $C_3 = 112$ depends only on the quantum numbers of the transition in question and $I_3^{(-3)}$ is an integral over momentum transfer given by

$$I_3^{(-3)} = \int_0^\infty \left[\int_0^\infty P_{nl_a} P_{n'l'_a} j_3(Kr) dr \right]^2 K^{-3} dK , \tag{51}$$

and where $j_3(Kr)$ is a spherical Bessel function of the first kind.

In order to interpolate the data in Table IX, use has been made of the interactive graphics program OMEUPS which is based on the method by Burgess and Tully [12] for interpolating and compacting collision strengths. Summaries of the method and the program are given elsewhere [13–15]. The originality of the method hinges on the use of scaling techniques which remove the main energy dependence from the data and map the entire range of E onto the interval [0,1]. The scaled or reduced variables are denoted by E_{red}, Ω_{red}. For an optically forbidden transition the data are reduced as

$$E_{red} = (E_i/E_{ij})/(E_j/E_{ij} + C) , \tag{52}$$

$$\Omega_{red} = \Omega , \tag{53}$$

where $C > 0$ and $E_j = E_i - E_{ij}$ is the free-electron energy

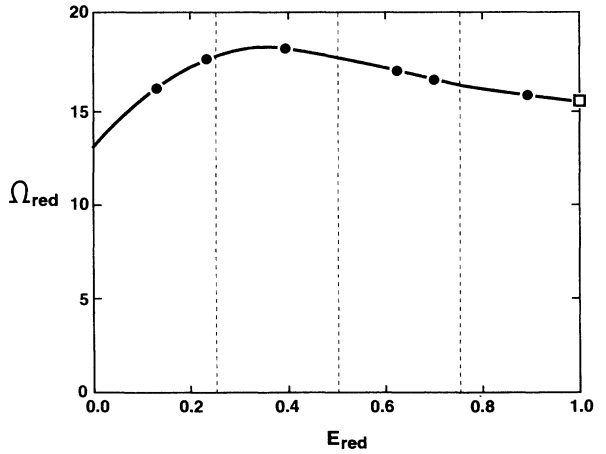

FIG. 2. Scaled total-collision strength Ω_{red} for the $5s$-$4f$ transition in Ca^+, plotted against scaled energy E_{red}. ●, reduced data; ——, spline fit to the reduced data; □, Born limit. Adjustable parameter $C=4$ with knot values 13.04, 17.78, 17.88, 16.32, 15.46.

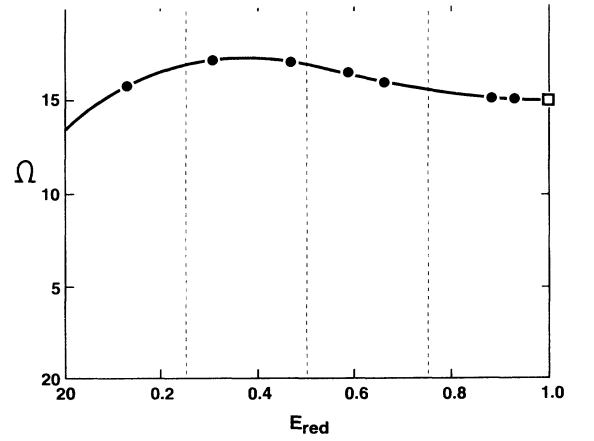

FIG. 4. Scaled total-collision strength Ω_{red} for the $6s$-$4f$ transition in Sr^+, plotted against scaled energy E_{red}. ●, reduced data; ——, spline fit to the reduced data; □, Born limit. Adjustable parameter $C=6$ with knot values 13.26, 16.81, 16.77, 15.45, 14.87.

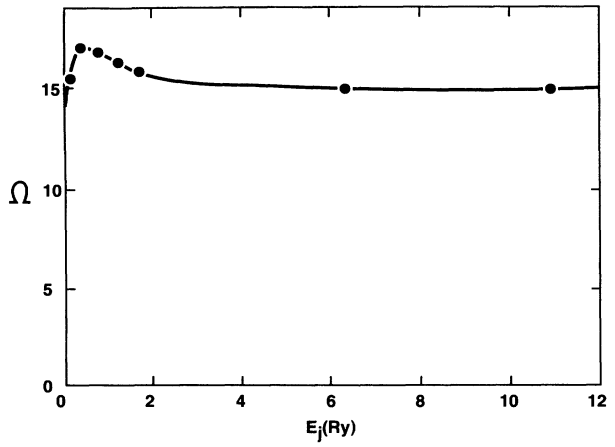

FIG. 5. Total-collision strength Ω for the 5*s*-4*f* transition in Ca^+, plotted against electron energy after excitation E_j. ●, original data; ——, spline fit to the data.

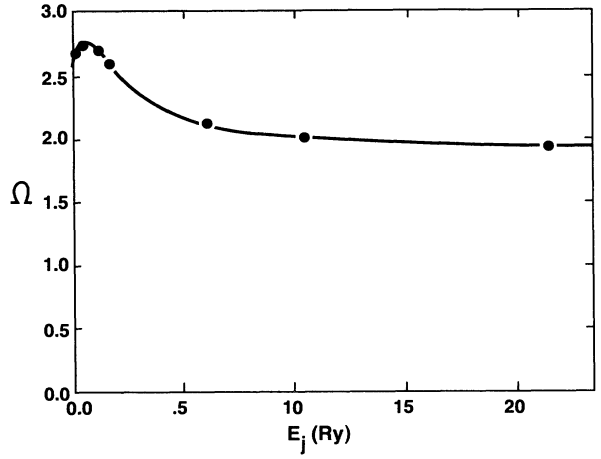

FIG. 6. Total-collision strength Ω for the 5*s*-4*f* transition in Sr^+, plotted against electron energy after excitation E_j. ●, original data; ——, spline fit to the data.

after excitation. The parameter C depends on the transition; its value can be adjusted in order to optimize the plot of Ω_{red} prior to making a spline fit. The spline curve is defined by its values at the five equally spaced knots. A short program for the spline interpolation and extrapolation is given in Appendix C of a previous publication [13]. Figures 1–4 are examples, produced by an IBM PS/2 of the reduced data and spline fit to the reduced data for the *s*-*f* transitions in Ca^+ and Sr^+. A graphical comparison of the original data (Ω) and the spline fit, which represents the data typically to an accuracy of a fraction of a percent, is shown in Figs. 5 and 6. It is worth mentioning that, for the transition 5*s*-4*f* in Ca^+, the interpolation procedure of OMEUPS gives a collision strength of $\Omega=14.88$ for the energy point $E_j=22.469\,11$ Ry as compared to $\Omega=15.06$ shown in Table VI.

IV. CONCLUSIONS

The convergence of the sum over partial-collision strengths, for excitation of octupole transitions in positive ions, has been examined formally and by sample calculations on Sr^+ and Ca^+. Two different methods, based on the Coulomb-Bethe approximation, were obtained to complete the summation over the infinite partial-wave contributions. The first method, referred to as the geometric-series method, makes use of the findings in this paper, shared by dipole and quadrupole transitions, that the sum over partial-collision strengths is asymptotic to a geometric series of ratio E_j/E_i, where E_i and E_j are the initial and final energies of the colliding electron, respectively. The second method or method of sums of reciprocal powers, avoids the numerical difficulties encountered at large colliding electron energies ($E_j/E_i\sim 1$) when the convergence of the sum to the geometric series is rather slow.

These methods have been incorporated into the calculation of total-collision strengths for electron-impact excitation of *s*-*f* transitions in Sr^+ and Ca^+ ions. These total-collision strengths, calculated in the nonexchange Coulomb-distorted-wave approximation CDWII, have been analyzed using the OMEUPS method which removes the main energy dependence from the data and maps the entire range onto the interval [0,1]. The OMEUPS method also verifies that the analytic formulas derived to estimate the contribution to the total-collision strength from large values of angular momentum give data with the correct high-energy behavior.

ACKNOWLEDGMENTS

This work was supported in part by the Natural Sciences and Engineering Research Council of Canada. I am grateful to A. Burgess for the use of some of his subroutines.

[1] I. V. Hertel and K. J. Ross, J. Phys. B **1**, 697 (1968).
[2] R. H. Garstang, J. Phys. B **1**, 847 (1968).
[3] A. Burgess, D. G. Hummer, and J. A. Tully, Philos. Trans. R. Soc. London, Ser. A **266**, 225 (1970).
[4] A. Burgess, J. Phys. B **7**, L364 (1974).
[5] M. C. Chidichimo and S. P. Haigh, Phys. Rev. A **39**, 4991 (1989).
[6] D. M. Brink and G. R. Satchler, *Angular Momentum*, 2nd ed. (Oxford University Press, Oxford, 1968), p. 136.
[7] K. Alder, A. Bohr, T. Huus, B. Mottelson, and A. Winther, Rev. Mod. Phys. **28**, 432 (1956).
[8] G. N. Watson, *Theory of Bessel Functions*, 2nd ed. (Cambridge University Press, Cambridge, England, 1944), p. 401.

[9] B. W. Char, K. O. Geddes, G. H. Gonnet, M. B. Monagan, and S. M. Watt, *The Maple Reference Manual,* 5th ed. (WATCOM, Waterloo, Canada, 1988).
[10] M. C. Chidichimo, Phys. Rev. A **38**, 6107 (1988).
[11] M. C. Chidichimo, Phys. Rev. A **37**, 4097 (1988).
[12] A. Burgess and J. A. Tully, Astron. Astrophys. (to be published).
[13] A. Burgess, H. E. Mason, and J. A. Tully, Astron. Astrophys. **217**, 319 (1989).
[14] A. Burgess, M. C. Chidichimo, and J. A. Tully, Phys. Rev. A **40**, 451 (1989).
[15] A. Burgess, M. C. Chidichimo, H. E. Mason, and J. A. Tully, J. Phys. Paris Colloq. Suppl. II **1**, C1-303 (1991).